Russian Geology and Geophysics © 2019, V.S. Sobolev IGM, Siberian Branch of the RAS
Vol. 60, No. 8, pp. 833–844, 2019 *DOI:10.15372/RGG2019052* *Geologiya i Geofizika*

Dynamics of Metasomatic Transformation of the Rocks of the Lithospheric Mantle and Earth's Crust in Deep-Fault Zones Controlling the Siberian Platform Trap Magmatism

V.N. Sharapov [a,b,] ✉, M.P. Mazurov [a], K.V. Chudnenko [c], K.E. Sorokin [a]

[a] *V.S. Sobolev Institute of Geology and Mineralogy, Siberian Branch of the Russian Academy of Sciences, pr. Akademika Koptyuga 3, Novosibirsk, 630090, Russia*

[b] *Novosibirsk State University, ul. Pirogova 2, Novosibirsk, 630090, Russia*

[c] *A.P. Vinogradov Institute of Geochemistry, Siberian Branch of the Russian Academy of Sciences, ul. Favorskogo 1a, Irkutsk, 664033, Russia*

Received 16 January 2018; accepted 8 November 2018

Abstract—For a multirate approximation, we have determined the dynamics of rock heating by a magmatic-fluid flow in a flat permeable zone cutting the cratonic lithosphere of the Siberian Platform from a magma chamber at a depth of 50 km to the Earth's surface. This dynamics is compared with the dynamics of infiltration metasomatism in a three-layer lithosphere section: (1) harzburgitic mantle (depth 50–40 km), (2) crystalline basement (39–7 km), whose composition was simulated by the section of rocks hosting the skarn deposits of the Aldan Shield, and (3) platform cover (6–0 km), with its simplified rock compositions specified on the basis of the rock compositions in the southern and northern parts of the trap area of the Siberian Platform. Numerical modeling of the metasomatic transformation of rocks was performed in a multireservoir flow reactor, using the Selektor software. The initial composition of fluids in a magmatic source varied from highly reduced (water–methane) to ordinary (water–acid) (lg p_{O_2} from –13.0 to –12.0). The obtained balances of the interacting phases show no significant change in the mass of aluminosilicate rocks in the mantle and Earth's crust sections and a significant loss of their mass under replacement of carbonate and sulfate deposits.

Keywords: traps, modeling, fluids, infiltration metasomatism, Siberian Platform

INTRODUCTION

Trap metallogeny of the Siberian Platform correlates with the parameters of crustal rock assimilation by basic magmas and their interactions with the platform cover fluids (Naldrett, 2003; Polyakov, 2009; Ryabov et al., 2018). The scope of these phenomena was determined by studying magmatogenic fluid systems coupled with the trap intrusions of Siberian Platform (Pavlov and Pek, 1979; Mazurov, 1985; Pukhnarevich, 1986; Sharapov et al., 1992; Aplonov, 2001; Turovtsev, 2002; etc.). It follows from these data that basic melt intrusions in the Siberian Platform cover caused transformations of both magmatic fluids and hosting rocks, which contained porous fluids, on various scales. A comprehensive review of qualitative "basic melt—evaporite" interaction patterns and formation mechanisms of orthomagmatic ore-forming systems is presented in (Warren, 2016). However, some of the discovered evolution processes of the Siberian Platform fluid systems did not fit the descriptions of local-contact interactions between specific magmatic bodies and platform cover rocks (Spiridonov and Gitsenko, 2009; Ryabov et al., 2018). A possible nature of some of the noted "nonnear-contact" phenomena is discussed in the present paper.

ON THE PROBLEM OF POSSIBLE FORMS OF MANIFESTATION AND SCALES OF DEEP FLUID FLOWS IN THE CRYSTALLINE BASEMENT AND PLATFORM COVER UNDERLYING THE EFFUSIVE SECTIONS OF SIBERIAN TRAPS

The problem considered below is a part of the larger issue discussed in the Russian scientific literature from the middle of the previous century to recent years, which involves convective heat and mass exchange processes at various levels between the upper mantle and the lithosphere of the Asian continent in its post-Proterozoic history. In terms of content, the models involved are based on the series of infiltration metasomatism processes in the Earth's crust described in a systematic fashion in (Zharikov et al., 1998). Model reconstructions are decomposed into formalized systems of significantly different scales with significantly different levels of mathematical detail available in the present century (Letnikov, 2003, 2006, 2015; Sharapov et al., 2007;

✉ Corresponding author.
E-mail adress: vik@igm.nsc.ru (V.N. Sharapov)

Polyakov, 2009; Chudnenko, 2010; Cherepanova et al., 2015). Numerical models of heat and mass exchange dynamics dealing with metasomatism in the lithospheric mantle studied for the Siberian Platform and its magmatic and above-asthenospheric fluid systems (Sharapov, 2005; Sharapov et al., 2010, 2015). Here, qualitative thermodynamic models (Letnikov, 2003, 2006) and quantitative assessments of nonisothermal infiltration metasomatism in the steady-state approximation (Sharapov, 2005) turned out to be inconsistent in terms of possible scales of sublimation and growth of metasomatized rock mass at the interface between the lithospheric mantle and the Earth's crust. Hence, the necessity to refine the said quantitative model and consider the infiltration metasomatism processes in the lithospheric mantle and the Earth's crust simultaneously based on a more consistent description of hydrodynamics in the permeable zone (Sorokin, 2016), than a quasi-2D approximation (Bessonova et al., 2010) implemented in the cited papers.

Quantitative description of these phenomena under the craton by means of the reactor scheme of the Selector software (Karpov et al., 1994, 2001), combined with the description of convective heating dynamics in the zone in the lithospheric mantle and the Earth's crust, makes it possible to obtain the most multidimensional picture of mineral composition and phase balance in the metasomatic column areas for the equilibrium approximation. The idea boils down to combining the most accurate description of the multirate approximation of nonisothermal filtration hydrodynamics of the magmatic fluid in the permeable zone overlaying its source with the description of the balanced heterophase fluid-rock interaction within the consecutive chain of hydraulically linked equivalent fragments (reactors). The equilibrium of the interacting media is solved assuming the Gibbs-Korzhinsky principle of instantaneous reaction rate for the fluid-rock interactions at all reactor points and the lossless transfer of the reacted fluid between the reactors. The upper estimate obtained this way makes it possible to register the maximum possible variations in input-output parameters of the major and some trace components for the whole modeled system or its specific part at any time during the system's evolution.

The present state of the infiltration metasomatism theory and its applications are reflected in papers by Russian researchers (Letnikov, 2015). The earlier analysis of steady-state nonisothermal models of these processes for the West Siberian plate (Sharapov, 2005) showed that fluid-related physicochemical destruction phenomena were not observed in crustal, primarily aluminosilicate, rock masses (Letnikov, 2003, 2006), including both the upper horizons of the lithospheric mantle and the rocks of the lower Earth's crust. These findings agree with the geophysical data on the structure of the Earth's crust and the upper mantle in the West Siberian Plate region (Vitte et al., 2009). Metasomatic propylitization of tuffs and lavas was discovered in the fault zones controlling the evolution of effusive traps in the Permian–Triassic trap formation of the West Siberian Plate (Saraev et al., 2009; Berzin et al., 2016). Ubiquitous occurrences of volcanic suites in above-ore strata, where magmatic sulfide deposits of the low-temperature fluid systems develop, are observed within the Permian–Triassic trap formation in the Siberian Platform (Spiridonov and Gritsenko, 2009; Ryabov et al., 2018). A rather consistent description of the current state of fluid systems in the Siberian Platform cover is available (Samsonov and Larichev, 2008; Gazhula, 2008; Bukaty, 2009; Novikov, 2009; Archagov, 2010; Gordeeva, 2011; etc.), which makes it possible to speculate on the effect of neotectonic faults on zoning of porous fluid compositions in the platform cover section. The additional information on the behavior of fluid systems in the current spreading zones makes it possible to assess the specificity of the system modeled below.

ON THERMODYNAMIC PARAMETERS OF CURRENT MAGMATOGENIC FLUID SYSTEMS IN INTRAPLATE SPREADING ZONES

To state the problem of heat and mass exchange paleodynamics in the Earth's crust underlying the shield volcanoes in the intraplate spreading zones, we require information on temperatures and compositions of magmatic fluids in the active thermal systems of the subaerial discharge zones of thermal systems overlaying the deep faults (Sorey and Colvard, 1996; Gudmundsson, 2000; Saemundsson, 2013). In terms of maximum temperature, three types of endogenic fluids are in the depth interval of about 1 km: (1) $T > 150$ °C; (2) $T > 200$ °C; (3) $T > 370$ °C. The genesis of fluids is identified in all cases as a mixture of pore fracture waters and magmatic gases in different ratios. No thermal systems with temperatures over 200 °C were observed in the synrift structures, where only basic volcanism was manifested, and no cuirasses were present in the surface hot water discharge zones. Thus, fluid system manifestations in the West Siberian Plate traps are atypical for the recent crustal sections with the prevalence of effusive basic igneous rocks in terms of scale and metallogenic productivity. High-temperature fluid systems occur in the areas of spreading zones, where acid volcanism is present as well (Saemundsson, 2013). However, mineralization parameters of lava sections overlaying the salt rock masses in the Siberian Platform cover appear to be radically different (Spiridonov and Gritsenko, 2009; Ryabov et al., 2018). Specific structural features of pore fracture salt brines (see above) and the absence of mineralization zoning above the salt in fractures in the sedimentary cover rocks peculiar for the salt deposit basins with no igneous intrusions were discovered in the Siberian Platform cover (Popov et al., 2016).

PROBLEM STATEMENT

Tectonic control of the magmatogenic systems of the Siberian Platform trap formation is determined using the mul-

tiscale fault grid with a step of about 40 km, where the locations of ore clusters and individual diatremes are indicated by intersections of major faults (Varand, 1974; Pukhnarevich, 1986; Sapronov, 1986; Gordeeva, 2011). The hydrodynamic field of lithospheric fluids filtered by this fault grid shows peculiar 3D features (Person et al., 2012). The full 3D numerical solution of the heat and mass transfer problem considering the nonisothermal heterophase fluid-rock interaction would require computational resources unavailable to the authors. Thus, 2D hydrodynamic model of fluid filtration from the mantle magmatic source with constant fluid flow rate is considered for a single vertical planar permeable zone with variable permeability and porosity of lithospheric rocks (Sorokin, 2016). It is integrated with the solution of the heterophase fluid-rock interaction problem (Bessonova et al., 2010; Sharapov et al., 2015). This problem statement does not take into account fluid losses outside the permeable zone and ignores the zoning of metamorphic rock transformations on these regions.

The data from (Mazurov, 1985; Pertsev and Kulakovsky, 1988; Kravchenko et al., 2010) were used as the initial data for analyzing granulite and amphibolite facies of these systems in the Siberian Platform. The following types of systems were modeled, accordingly structural control of magmatism:

1. Planar fluid conduits overlaying the roof of mantle magmatic chamber (at the depth of 50 km), where rock permeability varies from 10^{-16} to 10^{-13} m^2, and porosity from 1 to 4% (Table 1).

2. Fluid filtration hydrodynamics is approximated by compactable heterophase media (Sorokin, 2016).

3. Nonisothermal metasomatism dynamics is represented in the Selektor software via flow reactor modification (see above) (Table 1).

4. Simplified models for the platform cover sections were constructed based on (Kosygin, 1973), and for the crystalline basement based on (Pertsev and Kulakovsky, 1988; Kravchenko et al., 2010) (Tables 2, 3).

The mathematic statement of the infiltration metasomatism heat and mass exchange in the permeable zones of Siberian Platform is presented in previous papers (Polyakov, 2009; Sharapov et al., 2010, 2015). The following two types of effusive trap sections are considered below: (1) Lava shield of the volcanic trough developed over the carbonate rock mass with the salt-containing horizon. Sill intrusions are present in the crystalline basement cover (Table 2); (2) Lava shield volcano in the trough developed over the carbonate rock mass with sulfate deposit horizons (Table 3). Basic and basic-andesite intrusions are present in the carbonate rock masses of the platform cover, such as calcitites, dolomitized limestones, and dolomites with different trace contents of salt and aluminosilicate. Evolution times of deep fluid systems were assumed at about 100,000 year, which corresponds the establishment of the quasi-steady state of the temperature field in the permeable zones considered. The interaction of steady-state magmatogenic fluid sources were taken from calculations (Sharapov et al., 2007, 2010). The original fluid compositions in the mantle magmatic source varied as follows (mol): C(1-2), H(1-4), O(0-3), N(0.01), S(0.1—0.02), Cl(0.25—0.5), F(0.05—0.25), Si(0.1—0.5), Ti(0.01), Ca(0.1—0.2), Na(0.03), K(0.01—0.02) (Table 1).

The choice of the given variation ranges for the magmatogenic fluid compositions in the mantle source was informed by the results of the physicochemical study of possible fluid compositions in the mantle sources based on research into gas phase compositions in mantle xenolith minerals in kimberlites and diamonds (Sharapov et al., 2010). Considering the petrochemical parameters of the Siberian Platform traps (Sharapov et al., 2011) and the diagram (Green, 2006) showing ratios between fluid compositions and normal and alkaline basites in the mantle chamber

Table 1. Physical parameters of the media used in calculations

Parameter	Measurement unit	Symbol	Numerical value
Viscosity, magmatic fluid	Pa·s	μ_1	4.5×10^{-5}
Density, magmatic fluid	kg/m^3	ρ_1	120
Heat capacity, magmatic fluid	J/(kg·K)	c_1	3200
Thermal conductivity, magmatic fluid	W/(m·K)	λ_1	0.17
Fluid compressibility factor	m^2/N	β_2	8.07×10^{-5}
Density of the Earth's crust rocks	kg/m^3	ρ_r	2600
Density of lithospheric mantle rocks	kg/m^3	ρ_r	3000
Heat capacity of lithospheric rocks	J/(kg·K)	c_r	1000
Thermal conductivity of lithospheric rocks	W/(m·K)	λ_r	2.4
Heat transfer coefficient of the solution at the lateral fluid conduit surface	$W/(m^2 \cdot K)$	α_2	0.005–0.05
Fluid conduit length	*L*	km	50
Fluid conduit width	L_2	km	4
Effective porosity along the fluid conduit	%	*m*	0.01–0.04
Permeability variation along the fluid conduit	m^2	$K_{пр}$	10^{-16}–10^{-13}

Table 2. Model composition of rocks of the lithosphere section above the source of fluid, variant 1

Lithospheric structure	Rock	Depth, km	Rock composition, mol
Mantle	Dunite	50	Si(6.248)Ti(0.006)Al(0.082)Fe(0.583)Mn(0.023)Mg(10.705)Ca(0.112.52) Na(0.019)K(0.006) P(0.004)Cr(0.034)O(25.52)
		49	
		48	
		47	
		46	
		45	
		44	
		43	
		42	
	Carbonate	41	Si(0.0004)Al(0.0001)Fe(0.002)Mg(0.015)Ca(4.085) Na(0.047)C(1.2)O(5.1)
	Dunite	40	Si(6.248)Ti(0.006)Al(0.082)Fe(0.583)Mn(0.023)Mg(10.705)Ca(0.112) Na(0.019)K(0.006) P(0.004)H_2O(0.033)Cr(0.034)O(25.52)
		39	
	Carbonate	38	Si(0.0004)Al(0.0001)Fe(0.002)Mg(0.015)Ca(4.085) Na(0.047)C(1.9)O(5.1)
	Dolomite	37	Si(0.0004)Al(0.0001)Fe(0.002)Mg(0.815)Ca(8.885) Na(0.047)C(1.2)O(5.1)
		36	
	Basalt	35	Si(8.309)Ti(0.135)Al(1.806)Fe(0.751)Mn(0.024)Mg(1.268)Ca(1.807) Na(0.418)K(0.049) P(0.008)Cr(0.001)O(28.16)
		34	
	Carbonate	33	Si(0.0004)Al(0.0001)Fe(0.002)Mg(0.015)Ca(4.085) Na(0.047)C(1.9)O(5.1)
		32	
	Basalt	31	Si(8.309)Ti(0.135)Al(1.806)Fe(0.751)Mn(0.024)Mg(1.268)Ca(1.807) Na(0.418)K(0.049) P(0.008)Cr(0.001)O(28.16)
		30	
		29	
The Earth's crust	Basaltic andesite	28	Si(8.572)Ti(0.011)Al(0.281)Fe(0.687)Mn(0.021)Mg(5.856)Ca(1.682)
		27	
		26	
	Dolomite	25	Si(0.0004)Al(0.0001)Fe(0.002)Mg(0.815)Ca(8.885) Na(0.047)C(1.9)O(5.1)
		24	
	Carbonate	23	Si(0.0004)Al(0.0001)Fe(0.002)Mg(0.015)Ca(4.085) Na(0.047)C(1.9)O(5.1)
		22	
	Dolomite	21	Si(0.0004)Al(0.0001)Fe(0.002)Mg(0.815)Ca(8.885) Na(0.047)C(1.9)O(5.1)
		20	
		19	
	Basalt	18	Si(8.309)Ti(0.135)Al(1.806)Fe(0.751)Mn(0.024)Mg(1.268)Ca(1.807) Na(0.418)K(0.049) P(0.008)Cr(0.001)O(28.16)
		17	
		16	
	Dolomite	15	Si(0.0004)Al(0.0001)Fe(0.002)Mg(0.815)Ca(8.885) Na(0.047)C(1.9)O(5.1)
		14	
	Andesite	13	Si(9.201)Ti(0.146)Al(1.607)Fe(0.55)Mn(0.021)Mg(0.888)Ca(1.152) Na(0.655)K(0.225)P(0.026) Cr(0.001)O(28.29)
		12	
		11	
	Anhydrite	10	Si(0.45)Ti(0.03)Al(0.184)Fe(0.235)Mg(1.2)Ca(8)
	Dolomite	9	Si(3.36)Ti(0.053)Al(0.053)Fe(1.08)Mg(5.74)Ca(11.83) Na(0.047)C(1.9)O(5.1)
	Andesite	8	Si(9.201)Ti(0.146)Al(1.607)Fe(0.55)Mn(0.021)Mg(0.888)Ca(1.152)
Platform cover	Carbonate	7	Si(0.81)Ti(0.144)Al(0.16)Fe(0.073)Mg(1.44)Ca(15.1)
	Andesite	6	Si(9.201)Ti(0.146)Al(1.607)Fe(0.55)Mn(0.021)Mg(0.888)Ca(15.1) Na(0.655)K(0.225)P(0.026) Cr(0.001)O(28)
	Anhydrite	5	Si(0.0004)Al(0.0001)Fe(0.002)Mg(0.015)Ca(3.3) Na(22.44)K(3.2)S(5.12)C(0.01)O(21.4)
	Dolomite	4	Si(0.0004)Al(0.0001)Fe(0.002)Mg(0.815)Ca(8.885) Na(0.047)C(1.9)O(5.1)
	Carbonate	3	Si(0.0004)Al(0.0001)Fe(0.002)Mg(0.015)Ca(0.05) Na(0.047)C(1.9)O(5.1)
Lavas	Basalt	2	Si(8.309)Ti(0.135)Al(1.806)Fe(0.751)Mn(0.024)Mg(1.268)Ca(1.807) Na(0.418)K(0.049) P(0.008)Cr(0.001)O(28.16)
		1	

Table 3. Model composition of rocks of the lithosphere section above the source of fluid, variant 2

Lithospheric structure	Rock	Depth, km	Rock composition, mol
Mantle	Dunite	50	Si(6.248)Ti(0.006)Al(0.082)Fe(0.583)Mn(0.023)Mg(10.705)Ca(0.112.52) Na(0.019) K(0.006)P(0.004)Cr(0.034)O(25.52)
		49	
		48	
		47	
		46	
		45	
		44	
		43	
		42	
	Carbonate	41	Si(0.0004)Al(0.0001)Fe(0.002)Mg(0.015)Ca(4.085) Na(0.047)C(1.2)O(5.1)
	Dunite	40	Si(6.248)Ti(0.006)Al(0.082)Fe(0.583)Mn(0.023)Mg(10.705)Ca(0.112.52) Na(0.019) K(0.006)P(0.004)Cr(0.034)O(25.52)
		39	
	Websterite	38	Na(0.047)K(0.008)P(0.002)H_2O(0.056)Cr(0.018)O(27.8)
		37	
	Dolomite	36	Si(0.0004)Al(0.0001)Fe(0.002)Mg(0.815)Ca(8.885) Na(0.047)C(1.2)O(5.1)
		35	
		34	
	Carbonate	33	Si(0.0004)Al(0.0001)Fe(0.002)Mg(0.015)Ca(4.085) Na(0.047)C(1.2)O(5.1)
		32	
	Websterite	31	Si(7.28)Ti(0.023)Al(0.18)Fe(0.62)Mn(0.021)Mg(10.29)Ca(0.27)
		30	
The Earth's crust	Basalt	29	Si(8.309)Ti(0.135)Al(1.806)Fe(0.751)Mn(0.024)Mg(1.268)Ca(1.807) Na(0.418)K(0.049) P(0.008)Cr(0.001)O(28.16)
		28	
	Basaltic andesite	27	Si(9.201)Ti(0.146)Al(1.607)Fe(0.55)Mn(0.021)Mg(0.888)Ca(1.152) Na(0.655)K(0.225) P(0.026)H_2O(0.055)Cr(0.001)O(28.29)
	Dolomite	26	Si(0.0004)Al(0.0001)Fe(0.002)Mg(0.815)Ca(8.885) Na(0.047)C(1.2)O(5.1)
		25	
		24	
	Basalt	23	Si(8.309)Ti(0.135)Al(1.806)Fe(0.751)Mn(0.024)Mg(1.268)Ca(1.807) Na(0.418)K(0.049) P(0.008)Cr(0.001)O(28.16)
		22	
		21	
	Dolomite	20	Si(0.0004)Al(0.0001)Fe(0.002)Mg(0.815)Ca(8.885) Na(0.047)C(1.2)O(5.1)
		19	
		18	
	Basalt	17	Si(8.309)Ti(0.135)Al(1.806)Fe(0.751)Mn(0.024)Mg(1.268)Ca(1.807) Na(0.418)K(0.049) P(0.008)Cr(0.001)O(28.16)
		16	
		15	
		14	
	Basaltic andesite	13	Si(9.201)Ti(0.146)Al(1.607)Fe(0.55)Mn(0.021)Mg(0.888)Ca(1.152) Na(0.655)K(0.225) P(0.026)H_2O(0.055)Cr(0.001)O(28.29)
		12	
		11	
	Dolomite	10	Si(0.0004)Al(0.0001)Fe(0.002)Mg(0.815)Ca(8.885) Na(0.047)C(1.2)O(5.1)
Platform cover	Basaltic andesite	9	Si(9.201)Ti(0.146)Al(1.607)Fe(0.55)Mn(0.021)Mg(0.888)Ca(1.152) Na(0.655)K(0.225) P(0.026)H_2O (0.055)Cr(0.001)O(28.29)
	Dolomite	8	Si(0.0004)Al(0.0001)Fe(0.002)Mg(0.815)Ca(8.885) Na(0.047)C(1.2)O(5.1)
	Basaltic andesite	7	Si(9.201)Ti(0.146)Al(1.607)Fe(0.55)Mn(0.021)Mg(0.888)Ca(1.152) Na(0.655)K(0.225) P(0.026)H_2O(0.055)Cr(0,001)O(28.29)
	Dolomite	6	Si(0.0004)Al(0.0001)Fe(0.002)Mg(0.815)Ca(8.885) Na(0.047)C(1.2)O(5.1)
		5	
		4	
Lavas	Basalt	3	Si(8.309)Ti(0.135)Al(1.806)Fe(0.751)Mn(0.024)Mg(1.268)Ca(1.807) Na(0.418)K(0.049) P(0.008)Cr(0.001)O(28.16)
		2	
		1	

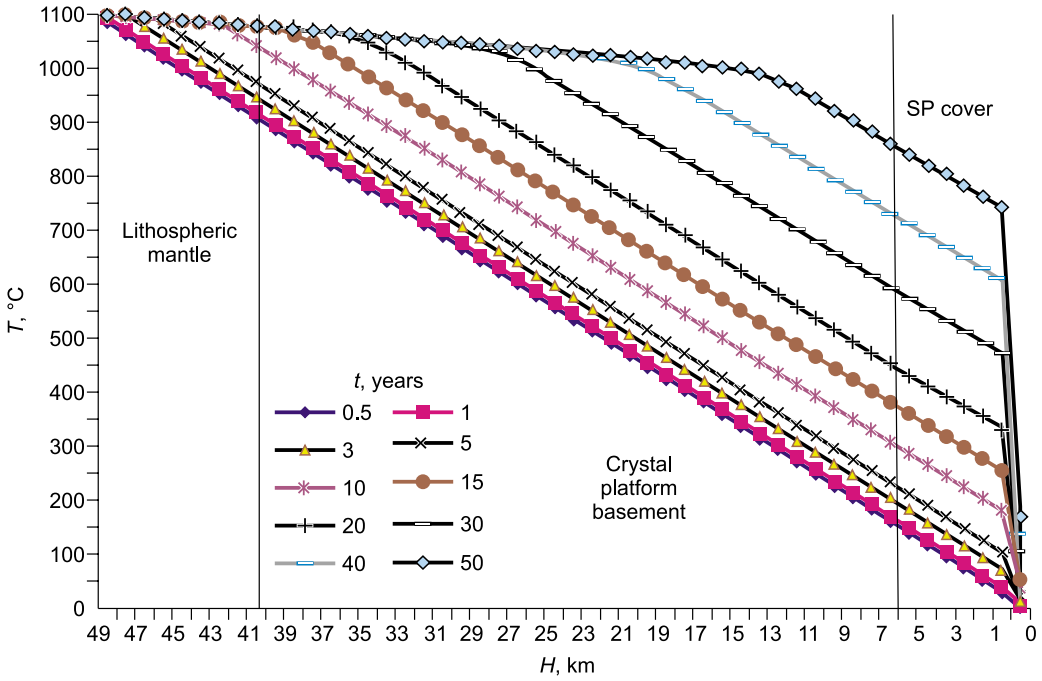

Fig. 1. Temperature dynamics in the permeable zone in time for the fluid system parameters (Table 1).

during the retrograde boiling of magma ($T \approx 1100$ °C), the presented relations make it possible to investigate the whole range of mantle fluid compositions according to (Green, 2006) and account for bulk quantities of individual compounds in temperature-dependent fluid compositions in individual reactors. Water-methane compositions, in which transfer of major components is majorized by the indicated Cl and F contents (see above) in the magmatic source, turn out to be prevalent fluids among the modeled compositions in the considered temperature and pressure range. Temperature dynamics in fluid flows in the permeable zone with thermophysical parameters of the modeled gas mixture compositions taken into account is presented in Fig. 1.

RESULTS OF NUMERICAL MODELING

Parameters of the balanced compositions of metasomatic rock transformation in the lithospheric mantle obtained in numerical experiments for the quasi-steady-state temperature distribution along the fluid filtration column section (Fig. 2) are similar to the data from (Sharapov et al., 2007,

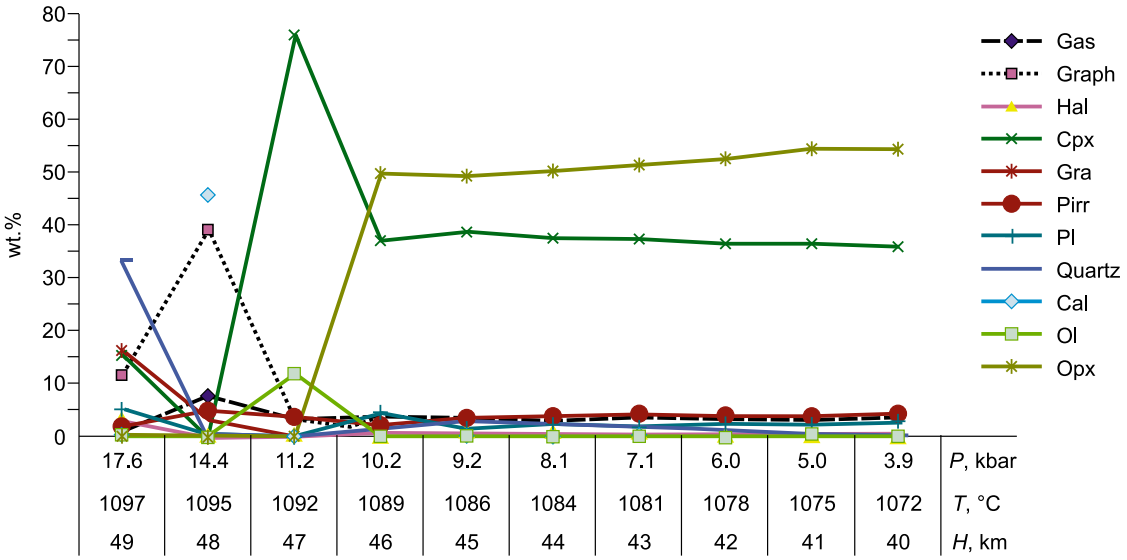

Fig. 2. Metasomatic column structure for the mantle part of the fluid system at t = 50 ka affected by the magmatogenic fluid C(1)H(2)O(3)S(0.1)N(0.01)Si(0.05)Al(0.1)Fe(0.1)Ca(0.1)Na(0.03)K(0.01).

2015). The symbols used in Fig. 2 and others are as follows: Amph, amphibole; Ang, anhydride; Brus, brucite; Cal, calcite; Clns, clinozoisite; Cpx, clinopyroxene; Gas, gas; Gra, garnet; Graph, graphite; Gps, gypsum; Hal, halite; Hem, hematite; Ksn, xonotlite; Mica, mica; Mont, montmorillonite; Mgt, magnetite; Ol, olivine; Opx, orthopyroxene; Per, periclase; Phlu, fluorite; Phos, phosphate; Pirr, pyrrhotite; Pl, plagioclase; Quartz, quartz; Rut, rutile; Sph, sphene; Sulph, sulfate. If we take into account the increase and decrease in masses of ultrabasic rocks below the Moho boundary or the lower-crustal aluminosilicate rocks (Sharapov et al., 2007), then no significant mass sublimation or growth phenomena are observed for the input major components in metasomatites at the considered times of fluid-rock interactions (Fig. 3). These results specify the ones obtained for steady-state temperature distributions presented in (Sharapov, 2005) with respect to spatial displacement of higher-temperature metasomatic facies towards the discharge zones. The obtained results of replacement of crystalline basement rocks of the deep granulite and amphibolite facies of the Siberian Platform (Fig. 4) qualitatively match with the available mineralogical descriptions of those from iron and noble metal deposits (Mazurov, 1985; Pertsev and Kulakovsky, 1988; Kravchenko et al., 2010). Numerical estimates of temperature transformation of rocks in deep fluid filtration areas in the permeable zones of the Earth's crust show that their geological evolution seemed to occur rather quickly, i.e., 35 ka, with the average thickness of the platform cover section being 6 km, and the temperature virtually varying from ≈ 140 to ≈ 860 °C at the lower boundary and from ≈ 4 to ≈ 220 °C in the subaerial discharge zone of the system. The

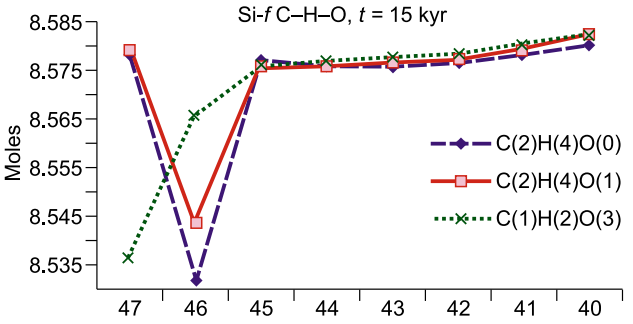

Fig. 3. Silicon content variation in the lithospheric mantle rocks affected by magmatogenic mantle fluids of various C–H–O compositions, the composition of the remaining components being constant: S(0.1)N(0.01)Si(0.05)Al(0.1)Fe(0.1)Ca(0.1)Na(0.03)K(0.01).

obtained data on mineralogical changes in rock compositions (Fig. 5) may act as a dynamic illustration of the evolution of new types of metasomatic rock formations and facies for various compositions of adjacent layers in the Earth's crust (Zharikov et al., 1998). It should be noted that the indicated temperature range covers the identical thermodynamic area, where near-ore rocks of the magnesium-skarn deposits of the Siberian craton are formed (Mazurov, 1985; Pertsev and Kulakovsky, 1988). Therefore, if mantle magmatogenic fluid flows occur in deep fault zones along the platform cover and crustal sections, then convective heating may be accompanied by development of metasomatic rocks of similar formation types, whose compositions will only be different in pressure dependences of minerals in the columns (Sobolev, 2017). The platform cover horizons formed by

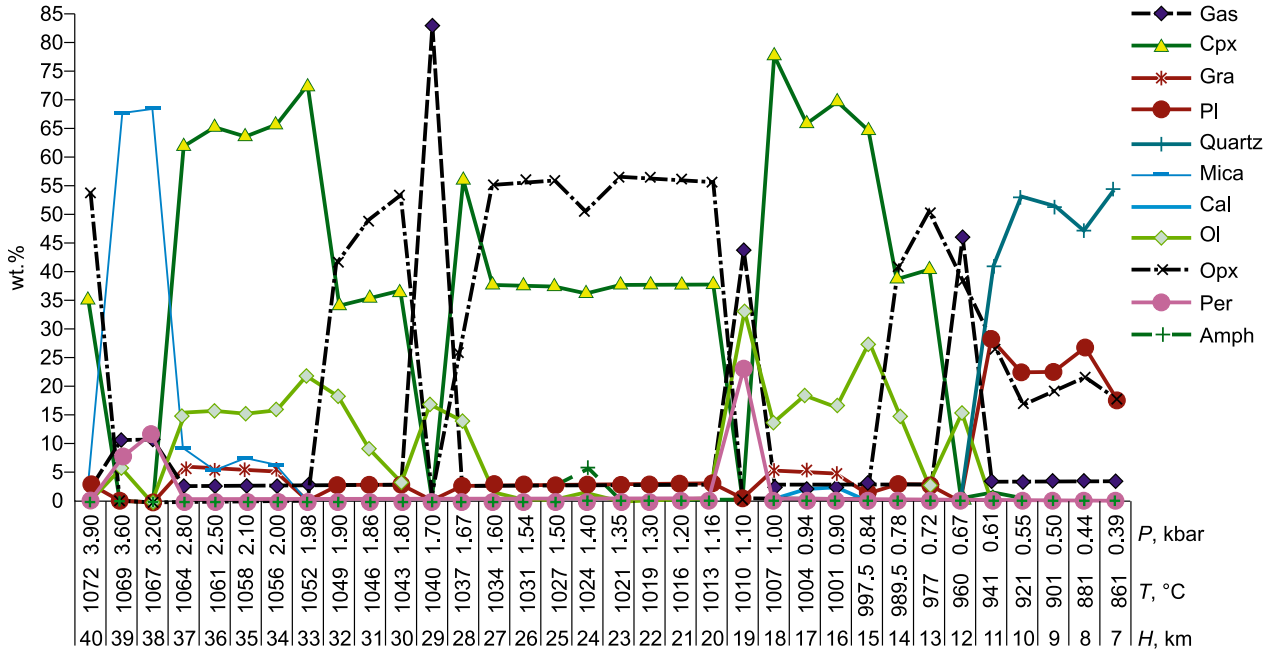

Fig. 4. Metasomatic column structure (Table 2) in crystalline basement rocks at interaction time of 50 ka affected by the fluid C(1)H(2)O(3) S(0.1)N(0.01)Si(0.05)Al(0.1)Fe(0.1)Ca(0.1)Na(0.03)K(0.01).

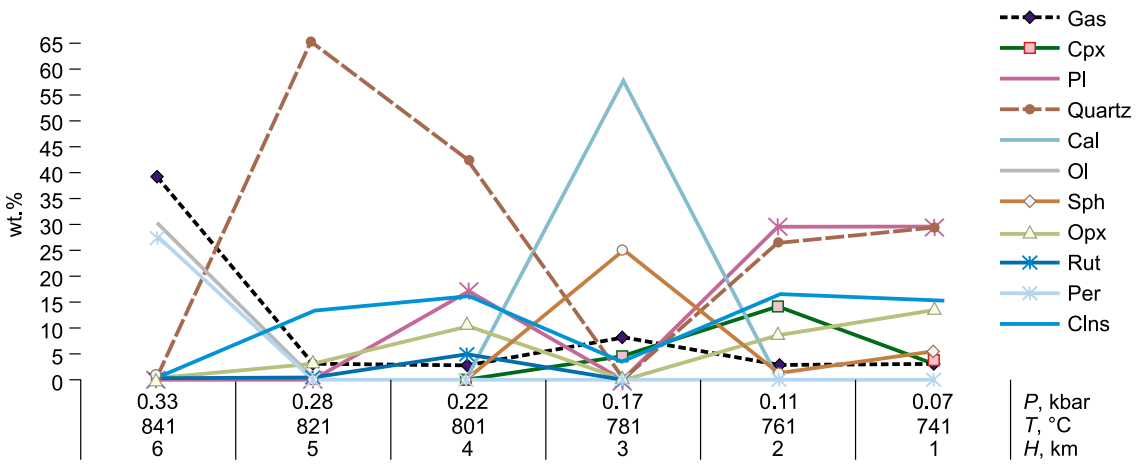

Fig. 5. Metasomatic column structure (Table 2) of the platform cover for the quasi-steady-state temperature distribution at t = 50 ka. Fluid composition is similar to Fig. 2.

salts have high chemical inertness, but also show rather high mechanical mobility at increasing temperatures in presence of fluids (Kosygin,1973; Bukaty, 2009).

The data on transformation of anhydrite deposit layers (Fig. 6) are the key addition to the interactions between evaporites and basic intrusions (Warren, 2016). These results make it possible to specify the presumable assimilation mechanisms of sulfur-containing deposits by the intruding basic melts with respect to different mineralizations of individual intrusions of the Norilsk and Kharaelakh troughs in the northwestern part of Siberian Platform (Li et al., 2009). The key factor in these metallogenic schemes being the possibility of dissolution of rather large volumes of sulfur-containing rocks in nonoverheated basic melts. The transformation scheme presented for the salt rock masses allows us to demonstrate the cause (Ryabov et al., 2018) of assimilation of large sulfur volumes from sedimentary rocks in the intermediate crustal magma chambers within the platform cover.

Thus, the initial compositions of sedimentary rocks within permeable zones undergo metasomatic transformations as follows: dolomitized limestones and dolomites are transformed into periclase marbles, and gypsums are replaced with carbonate marbles when the temperature rises above 380 °C. The obtained estimates of rock composition chang-

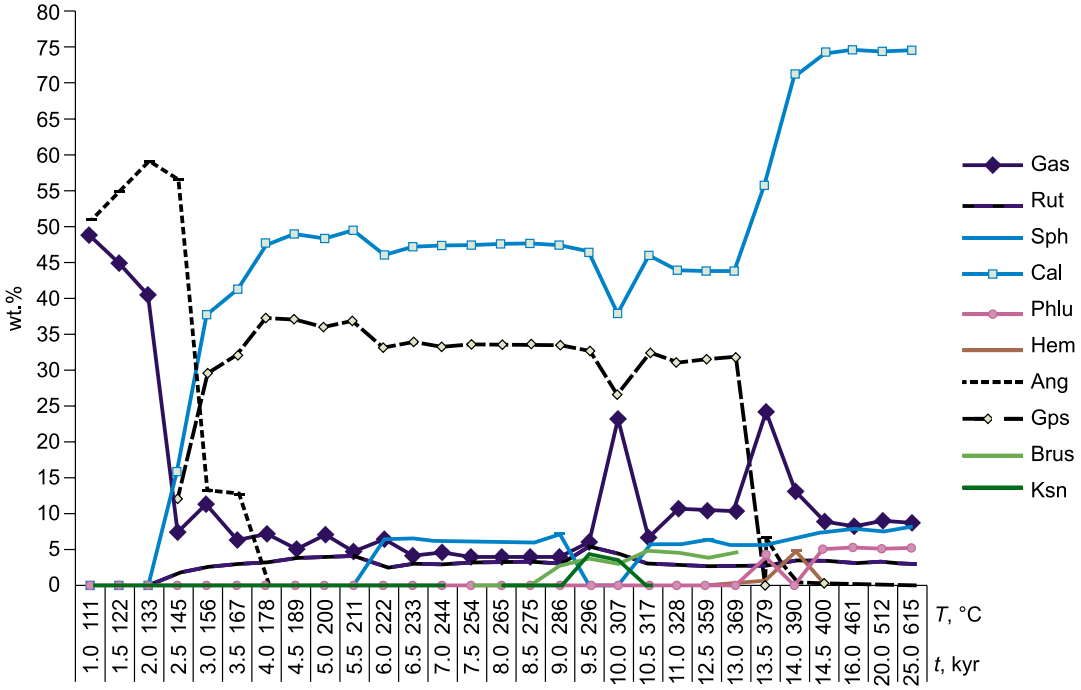

Fig. 6. Dynamics of balanced metasomatic transformation of the anhydrite layer affected by the fluid flow C(1)H(2)O(3)S(0.1)N(0.01)Si(0.05)Al(0.1)Fe(0.1)Ca(0.1)Na(0.03)K(0.01).

es in the platform cover agree in terms of thermodynamic prediction of possible locations of feeding zones for ore-bearing intrusions of the northwestern and northern escarpments of Siberian Platform and Taimyr (Dodin, 2002). They are in accordance with the available data on morphology, sizes, depth, and localization of the cover depressions in the northwestern and northern parts of the Siberian Platform (Kosygin, 1973; Afanasenkov et al., 2017). To understand the nature of the magmatic complexes in the northwestern and northern parts of the Siberian Platform (Dodin, 2002), the variations in petrogeochemical parameters of magmatic rocks (Ryabov et al., 2018), we may consider the mentioned transformation of anhydrite deposits into gypsum-bearing metasomatic rocks as a critical factor (Li et al., 2009), which determines the formation of unique magmatic sulfide rocks.

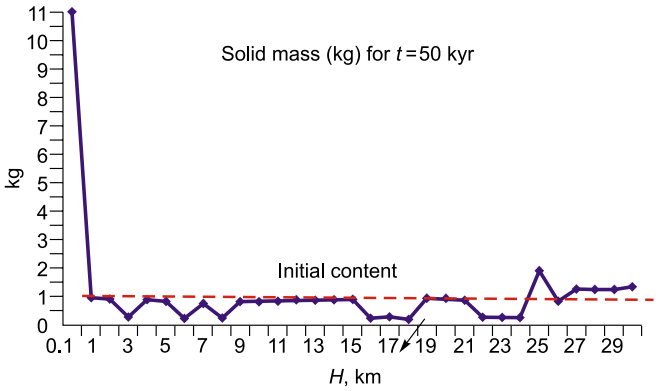

Fig. 7. Variations in solid phase mass content in the crystalline basement section (H = 30–7 km) and the platform cover (6–1 km) for the quasi-steady-state temperature distribution in the permeable zone.

ON POSSIBLE ENVIRONMENTAL AND GEOMORPHOLOGICAL CONSEQUENCES OF INFILTRATION TRANSFORMATION OF EVAPORITE ROCKS OF THE SIBERIAN PLATFORM COVER IN MANTLE-CRUST PERMEABLE ZONES

Consider the reaction mass balance of mantle fluid flows and platform cover rocks in permeable zones (Fig. 7). As follows from these data, metasomatic transformations of evaporites and intrusive bodies in evaporite sections are significantly different. In the former, positive or negative variations in masses of components are about 1–3 wt.%, whereas carbonate or sulfate rocks lose more than a half of their mass via gas phase separation. Major components are partially deposited in the form of low-temperature fillings (Fig. 8) of fractures and gas pores in the thermal system discharge zone and at the surfaces of volcanic edifices (Spiridonov and Gritsenko, 2009; Saraev et al., 2011), while the gas phase flows to the atmosphere. To interpret the nature of the Permian–Triassic environmental crisis, we primarily consider magmatic gas phase and dust discharge, which also include coal dust of the Permian coal deposits (Morgan et al., 2004; Payne et al., 2004; Sephton et al., 2005; Knoll et al., 2007; Reichow et al., 2009; Grasby et al., 2011; Shen and Bowring, 2014; etc.). It is worth noting that the considered recrystallization processes are accompanied by significant degassing and reduction in thickness of sedimentary rock mass subjected to metasomatic processing by fluids. Ore mineralization (sulfides, phosphates, titanates, fluorite, and hematite) in the variable temperature field occupies various niches and positions in the platform cover section during the temperature evolution of the fluid system (Fig. 9). However, as long as the integrated analysis of gas phase release in the gas phase discharge area is not performed for all active deep faults simultaneously, their role in the environmental crisis compared to other factors remains unclear. Nevertheless, we assume that the development of volcanic troughs and linear

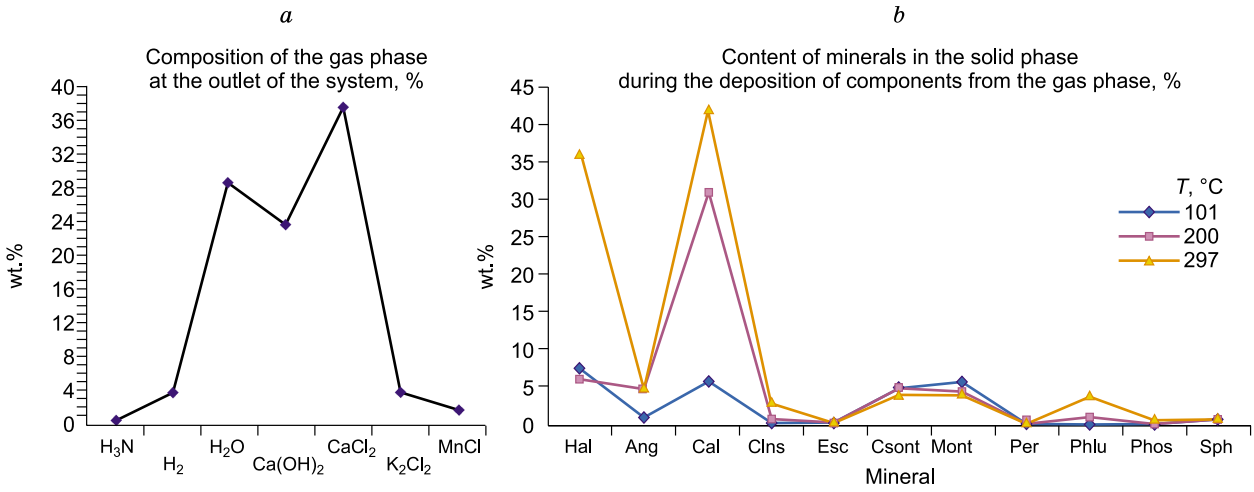

Fig. 8. Variations in compositions of the gas phase and mineral deposits of the gas phase in the subaerial fluid discharge zone. *a*, fluid phase composition in the discharge zone at the shield volcano surface above the permeable zone, fluid temperature is 298 °C; *b*, contents and compositions of mineral deposits in fractures below and at the fluid system discharge surface depending on fluid temperature.

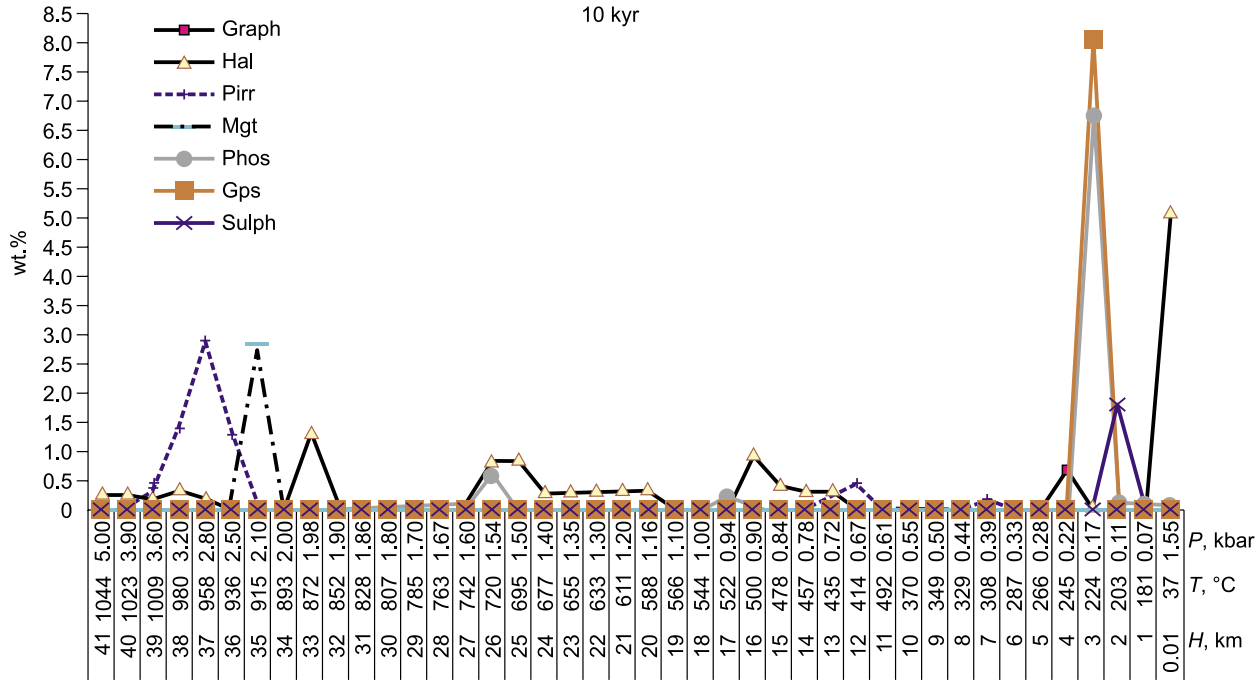

Fig. 9. Ore mineral and fracture zone filling distribution in the permeable zone of the Earth's crust.

grabens in the area where lava shields and dike belts manifest themselves, may among other things be attributed to the said factor.

CONCLUSIONS

The performed quantitative modeling of the interaction between the magmatogenic mantle fluid flows in regional fault zones makes it possible to understand the parameters of these processes in very limited areas. The obtained virtual quantitative estimates of possible directions and scales of metasomatic transformation of the crystalline basement rocks and the Siberian Platform cover in the deep fault zones make it possible to assume that scales and facies parameters of the considered phenomena should be significantly different within the relatively short recurrence periods of endogenous episodes on a geological event scale.

At the same time, the integrated effect of mantle fluids on the Siberian Platform cover and its regional scale remain unclear. Based on the cited results of studying hydrodynamic and hydrochemical parameters of pore fracture waters and salt brines in various oil- and gas-bearing regions of the Siberian Platform cover, we may conclude that hydrodynamic regime changes in the platform cover are only observed within large (global) tectonic wedges at the interfaces between plates or regional shear zones inside the plates. It seems that the difference in manifestations of "areal" hydrothermal systems between the Siberian Platform and the West Siberian Plate is more likely to be determined by differences in the tectonic conditions of trap intrusions, their distribution, and the amount of sills in the platform cover section in the scattered spreading zones, as well as by the composition of platform cover rocks in these plates, and by hydrocarbon and salt brine saturation of the pore space, rather than mantle fluid flows through permeable mantle-crust faults zones, which only have limited local effects. However, the discovered peculiarities of fluid flow effects play significant part in metallogenic variations in deep fault zones regarding the following:

1. Limited local occurrences of unique magmatic sulfide deposits.
2. Local formation of graphite deposits.
3. Significant scale of Iceland spar occurrences. The role of mantle fluid systems in terms of manifestations of magnomagnetite deposits is not yet clear as well.

The next step in studying the metallogenic role of these systems should be performing quantitative analysis of the development of mixed fluid systems, which appears inevitable in the considered situations.

The authors thank A.N. Vasilevsky and L.V. Vitte for the permission to use geophysical information in the analysis of structural control of the Permian-Triassic trap magmatism in the West Siberian Plate and the Siberian Platform, A.V. Mikheeva for the provided computational resources of the GIS-ENDDB system and consultation on its use, B.V. Lunev, Yu.V. Perepechko, V.V. Ryabov, and A.V. Tolstov for fruitful discussions of quantitative modeling problems considered in the paper. The contents of the paper were significantly improved thanks to critical comments and suggestions from A.S. Borisenko and O.P. Polyansky.

REFERENCES

Afanasenkov, A.P., Nikishin, A.M., Unger, A.V., 2017. Evolution history of Northwestern and Eastern Siberia in Meso-Cenozoic based on seismic data (Gydan, Ust'-Yenisei region). Geologiya Nefti i Gaza 1, 34–40.

Aplonov, V.S., 2001. Thermobarogeochemical Model of the Talnakh Platinum-Copper-Nickel Deposit [in Russian]. Saint Petersburg.

Archagov, V.S., 2010. Structure, oil-gas potential, and structural factors of zonal hydrocarbon clusters in ancient complexes of the Siberian Platform. Neftyanaya Geologiya. Teoriya i Praktika 5 (3), http://www/http.ru/4/41_2010pdf.

Berzin, S.V., Ivanov, K.S., Zaitseva, M.V., 2016. Permian–Triassic basalts from basement of the West Siberian basin from superdeep hole Yen-Yakhinskaya SG-7. Litosfera, No. 6, 117–128.

Bessonova, E.P., Sharapov, V.N., Chudnenko, K.V., Cherepanov, V.K., 2010. A new model of thermal and physicochemical dynamics for volcanogenic epithermal deposits (Asacha Deposit, Kamchatka). Dokl. Earth Sci. 431 (2), 453–457.

Bukaty, M.B., 2009. Groundwater geology of the western Siberian craton (implications for petroleum exploration). Russian Geology and Geophysics (Geologiya i Geofizika) 50 (11), 930–942 (1201–1217).

Cherepanova, V.K., Cherepanov, A.N., Sharapov, V.N., 2015. Modeling the Dynamics of Phase Change in Magmatic Systems and Metal Alloys [in Russian]. Novosibirsk. Gos. Tekhnik. Univ., Novosibirsk.

Chudnenko, K.V., 2010. Thermodynamic Modeling in Geochemistry: Theory, Algorithms, Software, and Application [in Russian]. Akad. Izd. Geo, Novosibirsk.

Dodin, D.A., 2002. Metallogeny of the Taimyr-Norilsk Region [in Russian]. Nauka, Saint Petersburg.

Gazhula, S.V., 2008. Peculiarities of trap magmatism in relation with conditions of hydrocarbon prospects in Siberian Platform. Neftyanaya Geologiya. Teoriya i Praktika 3, http://www.ngtp.ru/3//2008.pdf.

Golubev, V.S., 1981. Dynamics of Geochemical Processes [in Russian]. Nedra, Moscow.

Gordeeva, O.A., 2011. Oil and Gas Occurrence Prediction Criteria for the South Tunguska Area with high Evolution of Trap Magmatism (Lena–Tunguska Province). PhD Thesis [in Russian]. Novosibirsk, 2011.

Grasby, S.E., Sanei, H., Beauchamp, B., 2011. Catastrophic dispersion of coal fly ash into oceans during latest Permian extinction. Nature Geosci. 4, 104–107.

Green, D., 2006. Mantle Temperatures, http://www.MantlePlume.org.

Gudmundsson, A., 2000. Dynamics of volcanic systems in Iceland: Example of tectonism and volcanism at Juxtaposed Hot Spot and Mid-Ocean Ridge System. Annu. Rev. Earth Planet. Sci. 28, 107–140.

Karpov, I.K., Chudnenko, K.V., Bychinskii, V.A., 1994. SELEKTOR (Software Tool for Solving Chemical Equilibria via Thermodynamic Potential Minimization [in Russian]. IG SO RAN, Irkutsk.

Karpov, I.K., Chudnenko, K.V., Kravtsova, R.G., Bychinskii, V.A., 2001. Simulation of physicochemical processes of dissolution, transport, and deposition of gold in epithermal Au–Ag deposits in northeastern Russia. Geologiya i Geofizika (Russian Geology and Geophysics) 42 (3), 393–408 (379–394).

Knoll, H., Bambach, R.K., Payne, J.L., Pruss, S., Fisher, W.W., 2007. Paleophysiology and-Permian extinction. Earth Planet. Sci. Lett. 256 (3–4), 295–313.

Kosygin, Yu.A., 1973. Salt Tectonics of the Siberian Platform [in Russian]. Nauka, Novosibirsk.

Kravchenko, A.A., Smelov, A.P., Berezkin, V.I., Popov, N.V., 2010. Geology and genesis of gold-bearing Precambrian metabasites of the central part of the Aldan-Stanovoi Shield [in Russian]. Yakutsk, Ofset.

Letnikov, F.A., 2003. Magma-forming fluid systems of continental lithosphere. Geologiya i Geofizika (Russian Geology and Geophysics) 44 (12), 1262–1269 (1219–1225).

Letnikov, F.A., 2006. Fluids in endogenic processes and problems of metallogeny. Russian Geology and Geophysics (Geologiya i Geofizika) 47 (12), 1271–1281 (1296–1307).

Letnikov, F.A., 2015. Deep fluids in the continental lithosphere, in: Proc. Meet. "Fluid Regime of Endogenic Processes in the Continental Lithosphere" [in Russian]. IFZ SO RAN, Irkutsk, pp. 11–21.

Li, C., Ripley, E.M., Naldrett, A.J., 2009. A new genetic model for the giant Ni-Cu-PGE sulfide deposits associated with the Siberian flood basalts. Econ. Geol. 104 (2), 291–304.

Mazurov, M.P., 1985. Genetic Models of Skarn Iron Ore Formations [in Russian]. Nauka, Novosibirsk.

Morgan, J.P., Reston, T.J., Ranero, C.R., 2004. Contemporaneous mass extinctions, continental flood basalts, and "impact signals": are mantle plume-induced lithospheric gas explosions the causal link? Earth Planet. Sci. Lett. 217 (3–4), 263–284.

Naldrett, A.J., 2003. Magmatic Deposits of Sulfide Copper-Nickel and Platinum Ores [in Russian]. Sankt-Peterburg. Gos. Univ., Saint Petersburg.

Novikov, A.M., 2009. Salt Waters and Brines of the Olenek Cryoartesian Basin. PhD Thesis [in Russian]. Irkutsk.

Payne, J.L., Lehrmann, D.J., Wel, J., Orchard, M.J., Schrag, D.P., Knoll, A.H., 2004. Large pertrubations of the carbon cycle during recovery from the end-Permian extinction. Science 305, 506–509.

Person, M., Hoestra, A., Sweetkind, D., Stone, W., Cohen, D., Gable, C.W., Banerjee, A., 2012. Analitical and numerical models of hydrothermal fluid flow at fault intersections. Geofluids 12 (4), 312–326.

Pavlov, D.I., Pek, A.A., 1979. Formation of the Angara-Ilim-type iron deposits as a result of the thermal mobilization of formation salt brines by regional trap sill, in: Main Parameters of Natural Processes of Endogenic Ore Formation, Vol. 1 [in Russian]. Nauka, Novosibirsk, pp. 178–186.

Pertsev, N.N., Kulakovskii, A.L., 1988. Central Aldan Iron-Bearing Complex: Polymetamorphism and Structural Evolution [in Russian]. Nauka, Moscow.

Polyakov, G.V. (Ed.), 2009. Model-Based Analysis of Evolution of Continental Mantle-Crustal Ore-Forming Systems [in Russian]. ISO RAN, Novosibirsk.

Popov, V.G., Abdrakhmanov, R.F., Puchkov, V.N., 2016. Geodynamics and geochemistry processes of density convection in East European evaporite paleobasin. Litosfera, No. 3, 47–67.

Pukhnarevich, M.M., 1986. Formation Conditions of Endogenic Iron Deposits in the South of the Siberian Platform [in Russian]. Irkutsk. Gos. Univ., Irkutsk.

Reichow, M.K., Pringle, M.S., Al'Mukhamedov, A.I., Allen, M.B, Andreichev, V.I., Buslov, M.M., Davies, C.E., Fedoseev, G.S., Fitton, J.G., Medvedev, A.Ya., Mitchell, C., Puchkov, V.N., Safonova, I.Yi., Scott, R.A., Saunders, H., 2009. The timing and extent of eruption of the Siberian Traps large igneous province: Implications for the end-Permian environmental crisis. Earth Planet. Sci. Lett. 277 (1–2), 9–20.

Ryabov, V.V., Simonov, O.N., Snisar, S.G., Borovikov, A.A., 2018. The source of sulfur in sulfide deposits in the Siberian Platform traps (from isotope data). Russian Geology and Geophysics (Geologiya i Geofizika) 59 (8), 945–961 (453–466).

Saemundsson, K., 2013. Structural Geology—Tectonics, Volcanology and Geothermal Activity (Short Course VIII on Exploration for Geothermal Resources). ISOR, Reykyavik.

Samsonov, V.V., Larichev, A.I., 2008. Perspective oil-gas complexes of southern Siberian platform. Neftyanaya Geologiya. Teoriya i Praktika 3, http://www.ngtp.ru/4/43-2008.pdf.

Sapronov, N.L., 1986. Ancient Volcanic Structures in the South of the Tunguska Syneclise [in Russian]. Nauka, Novosibirsk.

Saraev, S.V., Baturina, T.P., Ponomarchuk, V.A., Travin, A.V., 2009. Permo-Triassic volcanics of the Koltogory–Urengoi rift of the West Siberian geosyneclise. Russian Geology and Geophysics (Geologiya i Geofizika) 50 (1), 1–14 (4–20).

Sephton, M., Looy, C., Brinkhts, H., Wingell, P.B., de Leeuw, J.W., Visscher, H., 2005. Catastrophic soil erosion during the end-Permian biotic crisis. Geology 33 (12), 941–944.

Sharapov, V.N., 2005. Evolution of mantle-crust fluid systems. Russian Geology and Geophysics (Geologiya i Geofizika) 46 (5), 451–461 (459–470).

Sharapov, V.N., Ione, K.G., Mazurov, M.P., Mysov, V.M., Perepechko, Yu.V., 2007. Geocatalysis and Evolution of Mantle-Crust Fluid Magmatic Systems [in Russian]. Akad. Izd. Geo, Novosibirsk.

Sharapov, V.N., Von-der-Flaass, G.S., Khomenko, A.V., 1992. Thermal reaction of a basite melt with the enclosing medium during its intrusion into beds of the Siberian Platform cover. Geologiya i Geofizika (Russian Geology and Geophysics) 33 (3), 43–56 (36–48).

Sharapov, V.N., Tomilenko, A.A., Perepechko, Yu.V., Chudnenko, K.V., Mazurov, M.P., 2010. The physicochemical dynamics of evolution of fluid above asthenosphere systems beneath the Siberian Platform. Russian Geology and Geophysics (Geologiya i Geofizika) 51 (9), 1037–1058 (1329–1355).

Sharapov, V.N., Cherepanov, A.N., Popov, V.N., Rakhmenkulova, I.F., 2011. Shield volcanoes of Siberian flood basalts: dynamics of lava sheets formation, in: Horizons in Earth Science Research, Vol. 4, pp. 61–98.

Sharapov, V.N., Chudnenko, K.V., Tomilenko, A.A., 2015. The physicochemical dynamics of carbonatization of the rocks of lithospheric mantle beneath the Siberian Platform. Russian Geology and Geophysics (Geologiya i Geofizika) 56 (5), 696–708 (980–905).

Shen, S.-zh., Bowring, S.A., 2014. The end-Permian mass extinction: a still unexplained catastrophe. Natl. Sci. Rev. 1 (4), 492–495.

Sobolev, N.V. (Ed.), 2017. The Nature and Models of Metamorphism [in Russian]. Nauka, Novosibirsk.

Soray, M.L., Colvard, E., 1996. Potential Effects of the Hawaii Geothermal Project on Ground-Water Resources of the Island Hawaii. US Geol. Surv., Menlo Park, California.

Sorokin, K.E., 2016. Modeling the Dynamics of Compressible Two-Phase Media in a Two-Speed Hydrodynamic Approximation. PhD Thesis [in Russian]. Novosibirsk.

Spiridonov, E.M., Gritsenko, Yu.D., 2009. Epigenetic Low-Grade Metamorphism and Co–Ni–Sb–As Mineralization in the Norilsk Ore Area [in Russian]. Nauchnyi Mir, Moscow.

Turovtsev, D.M., 2002. Contact Metamorphism of the Norilsk Intrusions [in Russian]. Nauchnyi Mir, Moscow.

Varand, E.L., 1974. Geology, Trap Magmatism, and Metallogeny of the Southern Part of the Lower Yenisei Metallogenic Area. PhD Thesis [in Russian]. Novosibirsk, 1974.

Vitte, L.V., Vasilevsky, A.N., Pavlov, B.V., 2009. Regional magnetic and gravity anomalies of the Siberian craton and their geological nature. Geofizicheskii Zhurnal 31 (6), 20–40.

Warren, J.K., 2016. Magma–evaporite–hydrothermal metal associations, in: Evaporites: A Geological Compendium. Springer Int. Publ., pp. 1591–1657.

Zharikov, V.A., Rusinov, V.L. (Eds.), 1998. Metosomatism and Metasomatic Rocks [in Russian]. Nauchnyi Mir, Moscow.

Editorial responsibility: A.S. Borisenko